Mini Review | Open Access

Catalysis, Energy and Environment

Zhou *et al. Catal. Energy Environ.* **2026**, *1*, 7 **DOI:**10.20517/cee.2026.06

Tribocatalysis: evolution toward efficient heterogeneous catalysis in aqueous solutions

Zeren Zhou[1], Wenqing Yao[2], Wanping Chen[1]

Keywords:
Tribocatalysis, semiconductors, metals, magnetic stirring, dye degradation, CO_2 reduction

Citation: Zhou, Z.; Yao, W.; Chen, W. Tribocatalysis: evolution toward efficient heterogeneous catalysis in aqueous solutions. *Catal. Energy Environ.* **2026**, *1*, 7. https://dx.doi.org/10.20517/cee.2026.06

Received: 11 Jul 2026
First Decision: 28 Jul 2026
Revised: 16 Sep 2026
Accepted: 17 Sep 2026
Published: 29 Sep 2026

Academic Editor:
Mingyang Xing
Copy Editor:
Shu-Yuan Duan
Production Editor:
Shu-Yuan Duan

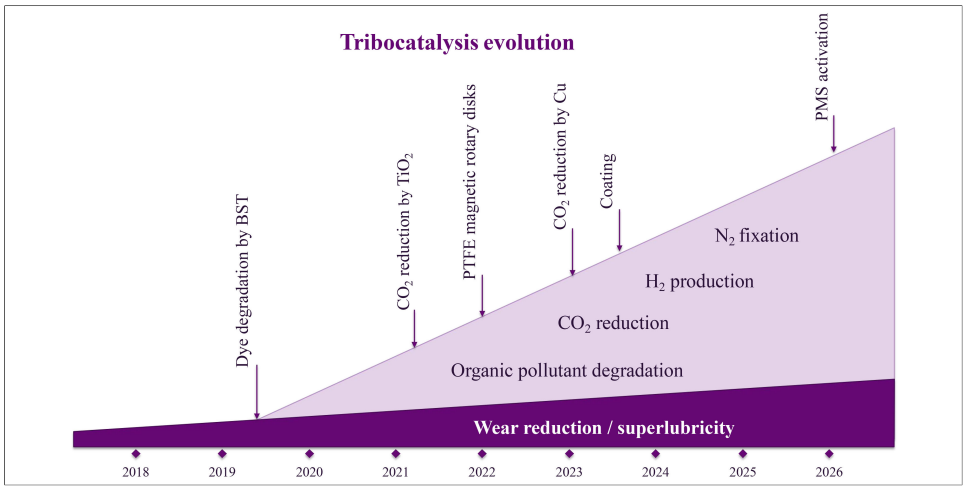

Abstract

Mechanochemistry and tribochemistry, together with their catalytic branches, mechanocatalysis and tribocatalysis, have traditionally focused on reactions between solids driven by low-frequency mechanical energy. Since the initial reports of organic-dye degradation by metal oxides under magnetic stirring, tribocatalysis has developed into an efficient form of heterogeneous catalysis in aqueous solutions. This mini-review summarizes the development of this emerging research direction. For semiconductors, a tribocatalytic mechanism has been established in which mechanical energy absorbed through friction excites electron-hole pairs. Several convenient and scalable strategies have proven particularly effective for enhancing semiconductor tribocatalysis, including replacing magnetic stirring rods with magnetic rotary disks, selecting highly crystalline semiconductors, optimizing friction pairs by coating the bottoms of reaction vessels, and coupling tribocatalysis with PMS/PDS. In addition to semiconductors, several bulk metals have been shown to convert H_2O and CO_2 into flammable gases through friction. For metallic materials, a distinct tribocatalytic mechanism has been proposed based on the formation of high-pressure micro-regions at frictional interfaces through elastic deformation of metals. Finally, we discuss common limitations in current tribocatalysis research and highlight the distinctive features that should guide future studies.

[1]School of Physics and Technology, Wuhan University, Wuhan 430072, Hubei, China.
[2]Department of Chemistry, Tsinghua University, Beijing 100084, China

Correspondence to: Prof. Wanping Chen, School of Physics and Technology, Wuhan University, Wuhan 430072, Hubei, China. E-mail: wpchen@whu.edu.cn

INTRODUCTION

Mechanical energy is a clean and abundant energy source in natural environments and plays an important role in the transition toward sustainability. Today, it is used as an energy input for chemical transformations such as biomass valorization and polymer depolymerization[1,2]. In fact, the use of mechanical forces to induce chemical reactions has been recognized for more than a century as an important subdiscipline of chemistry: mechanochemistry[3-6]. Similarly, tribochemistry specifically concerns chemical reactions in solids induced by frictional forces[7,8]. Given the central role of catalysis in chemistry, mechanocatalysis[9-11] and tribocatalysis[12,13] have naturally emerged as branches of mechanochemistry and tribochemistry, respectively.

Mechanical energy is particularly effective in initiating reactions between solids. Because biomass and polymers are often insoluble in common solvents, mechanochemistry and mechanocatalysis have been widely applied to biomass valorization and polymer depolymerization[1,2,14-17]. Research on tribochemistry and tribocatalysis, by contrast, has largely focused on reducing friction and even achieving superlubricity between solids[18-20]. To date, therefore, mechanochemistry and tribochemistry have primarily addressed mechanically induced reactions between solid-state reactants, whereas the use of mechanical energy to drive chemical reactions in solutions remains comparatively under-explored. It should also be noted that, perhaps due to the difficulty of scaling up, ultrasound is generally not considered a mechanical energy source within traditional mechanochemistry[5]; accordingly, ultrasound-induced reactions in solutions are not regarded as part of the field. Low-frequency mechanically stimulated reactions in solutions emerged much later. In 2019, tribocatalytic degradation of organic dyes was first reported using $Ba_{0.75}Sr_{0.25}TiO_3$ (BST) nanoparticles suspended in aqueous solutions and stimulated by magnetic stirring[21]. In that system, BST nanoparticles absorbed mechanical energy through friction and converted it into chemical energy that drove dye degradation in the surrounding aqueous solution. This work established a new form of low-frequency, mechanically driven heterogeneous catalysis in solutions. In subsequent years, tribocatalytic performance has improved markedly, and important mechanistic insights have also emerged, broadening both the theoretical and practical scope of mechanochemistry. To clarify the development in recent years, this mini-review summarizes the key milestones in the evolution of magnetic stirring-stimulated tribocatalysis toward efficient heterogeneous catalysis in aqueous solutions.

A TURNING POINT IN THE HISTORY OF MECHANOCATALYSIS AND TRIBOCATALYSIS

Mechanochemical reactions are commonly conducted in closed milling devices, where transient "hot spots" above 1,000 K can form at impact sites[22-24]. Because intermediate processes are difficult to monitor[25-27], these devices are often treated as "black boxes"[28,29], and mechanistic understanding of mechanochemistry, including mechanocatalysis, remains limited. In superlubricity-related tribocatalysis, the in situ formation of tribofilms under shear stress is highly sensitive to sliding speed, load, and humidity, further complicating mechanistic interpretation[30-32]. Figure 1 summarizes the annual numbers of publications on mechanocatalysis and tribocatalysis identified in Web of Science. Although both terms have been used for more than 30 years, annual publication numbers have remained low, especially when compared with photocatalysis, reflecting the challenges associated with understanding conventional mechanocatalysis and tribocatalysis.

By contrast, the history of tribocatalysis shows a pronounced turning point in 2019, after which publication numbers rose rapidly. As discussed below, this change coincides with the emergence of heterogeneous tribocatalysis in aqueous solutions. This development not only extended the scope of mechanochemistry to low-frequency friction-driven reactions in solutions, but also provided valuable mechanistic insights into tribocatalysis.

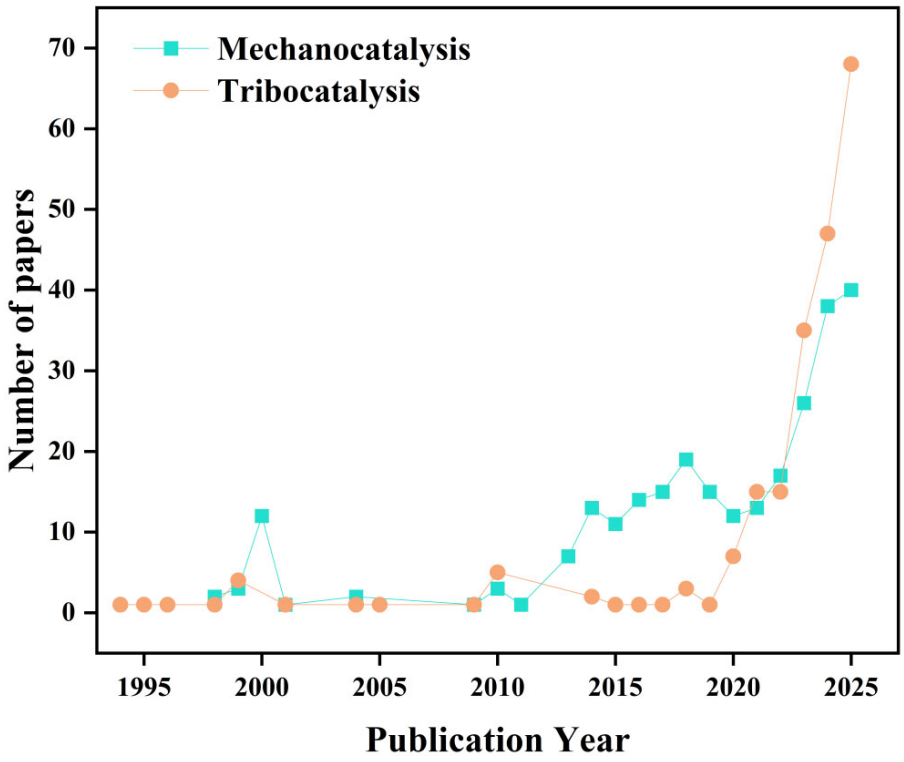

Figure 1. Publications on mechanocatalysis (using "mechanocataly*" or "mechano-cataly*" as topic) and on tribocatalysis (using "tribocataly*" or "tribo-cataly*" as topic) collected from https://www.webofscience.com/.

TRIBOCATALYSIS OF SEMICONDUCTORS IN AQUEOUS SOLUTIONS

Origin of tribocatalysis of semiconductors

Before 2019, several studies had already reported organic-dye degradation by metal oxides under magnetic stirring[33,34]. However, these observations were interpreted as piezocatalysis, based on the assumption that piezoelectric nanomaterials suspended in solutions were deformed by low-frequency mechanical stimulation[35]. In 2019, Li *et al.* reported a carefully designed experiment[21] demonstrating that BST nanoparticles located at the interface between polytetrafluoroethylene (PTFE) magnetic rods and the beaker bottom were responsible for the observed dye degradation under magnetic stirring. Based on these experimental results, the authors proposed a mechanism in which mechanical energy absorbed through friction excites electron-hole pairs in the BST nanoparticles[21]:

$$\mathrm{BST} \xrightarrow{\text{Friction}} \mathrm{BST} + \mathrm{h^+} + \mathrm{e^-} \quad (1)$$

As illustrated in Figure 2, the friction-excited electron-hole pairs diffuse to the BST surface, where they induce the formation of free radicals in the surrounding aqueous solution[21].

This mechanism establishes a direct electronic pathway by which friction can convert mechanical energy into chemical energy without requiring bulk heating or bond breaking in solids. To provide more direct evidence for friction-induced carrier excitation, silicon single crystals were used as a model semiconductor. As shown in Figure 3A and B, a 30 mg/L MO solution was rapidly decolorized by friction between Al_2O_3 nanoparticles and a silicon single crystal[36]. Because Al_2O_3 is widely regarded as an inert material under these conditions, this result provided clear evidence for the excitation of electron-hole pairs within silicon, as illustrated in Figure 3C. After the reaction, the silicon single crystal remained intact apart from surface scratches [Figure 3D]. The role of semiconductors in tribocatalysis has since attracted increasing attention, and dozens of

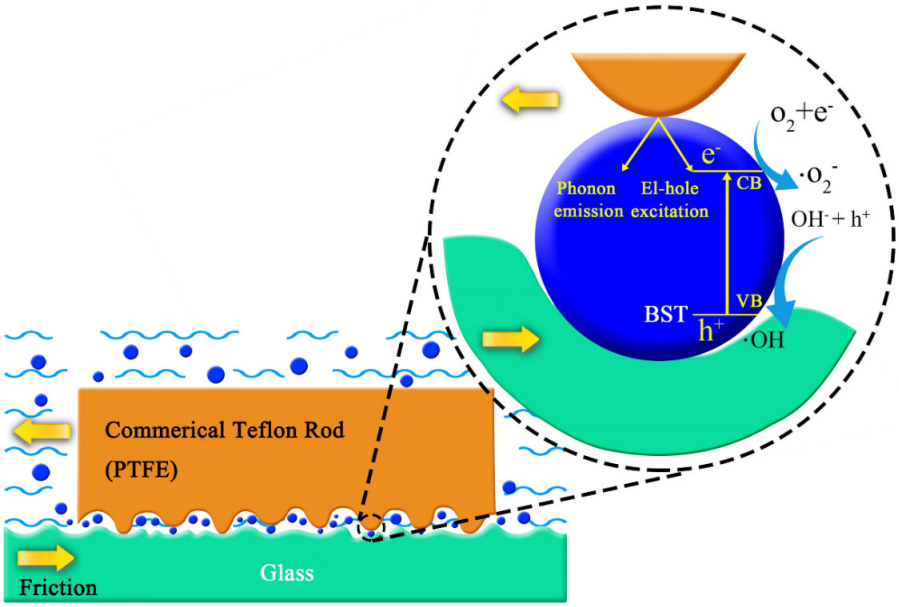

Figure 2. Mechanism for tribocatalytic degradation of organic pollutants by BST nanoparticles at the PTFE-glass interface during magnetic stirring: electron-hole pairs are excited in BST nanoparticles by mechanical energy absorbed through friction. Reprinted with permission from[21]. Copyright 2019 Elsevier. PTFE: Polytetrafluoroethylene; BST: $Ba_{0.75}Sr_{0.25}TiO_3$.

materials with semiconductor-type band structures have been investigated, including TiO_2[37-40], ZnO[41-43], $BaTiO_3$[44-47], $SrTiO_3$[48-50], CdS[51,52], GaN[53], SiC[54], Co_3O_4[55], NiO[56], and Fe_2O_3[57]. This expansion helps explain the sharp increase in tribocatalysis publications shown in Figure 1. Across these semiconductor systems, low-frequency magnetic stirring is the most common mechanical stimulation method, while representative applications include organic-pollutant degradation, H_2O/CO_2 conversion, nitrogen fixation, and related redox reactions. In the general mechanism discussed here, friction-induced electronic excitation in semiconductors generates charge carriers that participate directly in surface redox reactions or form reactive species; material-specific factors such as defects, piezoelectricity, and heterojunctions may further influence charge separation and transfer.

Enhancing strategies

When first reported, tribocatalysis was relatively weak, requiring 12 h of magnetic stirring to degrade a 5 mg/L RhB solution[21]. Under optimized conditions, however, modified magnetic stirring can now completely degrade RhB at concentrations as high as 500 mg/L within 24 h[40]. Thus, tribocatalytic performance has improved substantially over the past few years, and several enhancement strategies have proven particularly effective.

Magnetic rotary disks

Conventional magnetic stirring was used as the mechanical energy source in the earliest reports of tribocatalytic dye degradation and remains the most widely used method for supplying mechanical energy in tribocatalysis studies. To increase friction between PTFE magnetic stirring rods and the beaker bottom, multiple rods have been used simultaneously, producing a pronounced enhancement[21,37]. However, conventional magnetic stirring rods were not designed specifically for tribocatalysis, motivating the development of devices tailored to maximize frictional energy input.

To address this limitation, PTFE magnetic rotary disks were specifically designed. As shown in Figure 4[47], one face of a 35-mm-diameter PTFE disk contains a cross-shaped groove 4 mm wide, allowing suspended particles to enter the interface between the rotating disk and the beaker bottom. Eighteen magnets (5 mm × 5

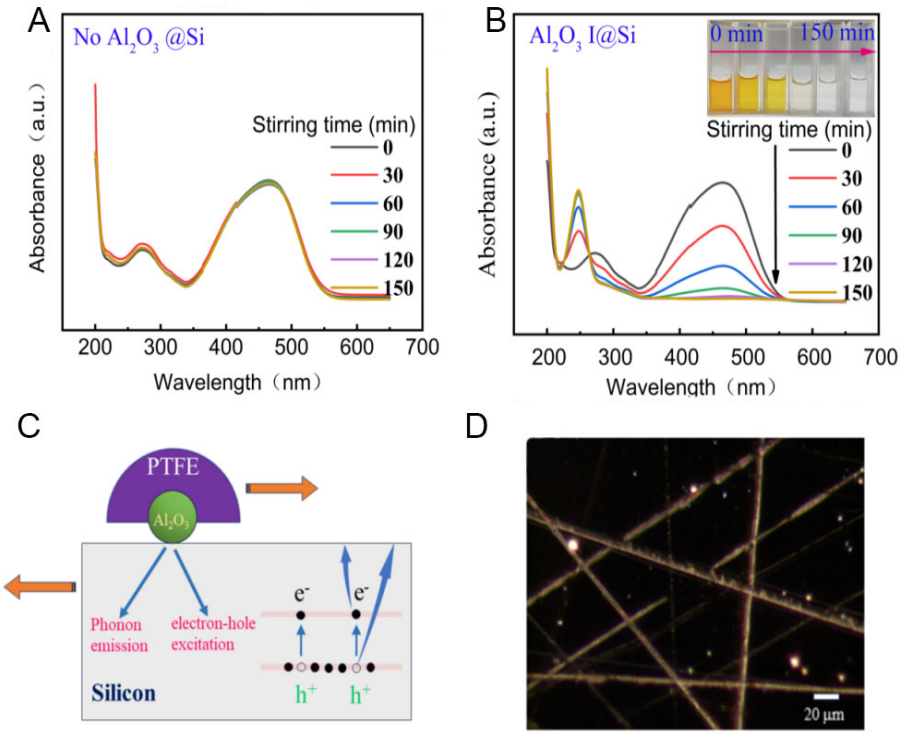

Figure 3. UV-Vis absorption spectra and color changes of a 30 mg/L MO solution during magnetic stirring in an Si-coated beaker: (A) without suspended particles; (B) with suspended Al_2O_3 I particles; (C) Schematic illustration of friction-induced excitation of electron-hole pairs in a silicon single crystal by Al_2O_3 particles; (D) Optical micrograph of the silicon single-crystal surface after 10 h of magnetic stirring with Al_2O_3 I particles. (A-D) are adapted with permission from[36]. Adhering to the CC BY 4.0 agreement. PTFE: Polytetrafluoroethylene; UV-Vis: ultraviolet-visible.

mm) are mounted inside the back cover, enabling the disk to be driven by a conventional magnetic stirrer. The relatively large number of magnets strengthens the magnetic coupling to the stirrer. Compared with a PTFE magnetic stirring rod[38], the disk provides a much larger contact area with the beaker bottom and exerts greater pressure on the interface, both of which enhance tribocatalysis. It is worth noting that disk mass, diameter, groove geometry, and contact area are all relevant device parameters because they determine the extent and stability of the friction interface.

PTFE magnetic rotary disks have since been adopted by several research groups for tribocatalytic degradation of organic dyes, with encouraging results. Figure 5, for example, illustrates their effect on the tribocatalytic degradation of a 10 mg/L RhB solution by TiO_2 nanoparticles[38]. Although using four PTFE magnetic rods simultaneously markedly improved the degradation rate, a single PTFE magnetic rotary disk produced the best performance. The advantage of PTFE magnetic rotary disks over PTFE magnetic stirring rods was so obvious that the comparison was not conducted for other organic dyes in that study[38]. This comparison highlights the importance of optimizing mechanical-energy input in tribocatalysis.

Tribocatalytic conversion of H_2O and CO_2 into flammable gases was first reported for TiO_2 nanoparticles stimulated by magnetic stirring with commercial PTFE magnetic stirring rods[37,58]. Gas production under those conditions was extremely low: after 50 h of magnetic stirring with four PTFE rods, only 8.98 ppm H_2, 2.61 ppm CH_4, and 30.04 ppm CO were produced[58]. By contrast, using a PTFE magnetic rotary disk, TiO_2 nanoparticles produced 40.5 ppm H_2, 9.1 ppm CH_4, and 29 ppm CO after 24 h[56]. Even more strikingly, NiO particles produced 12,868.8 ppm H_2 under the same conditions [Figure 6], more than 300 times the amount produced by TiO_2 nanoparticles. This result provides strong confirmation of the remarkable

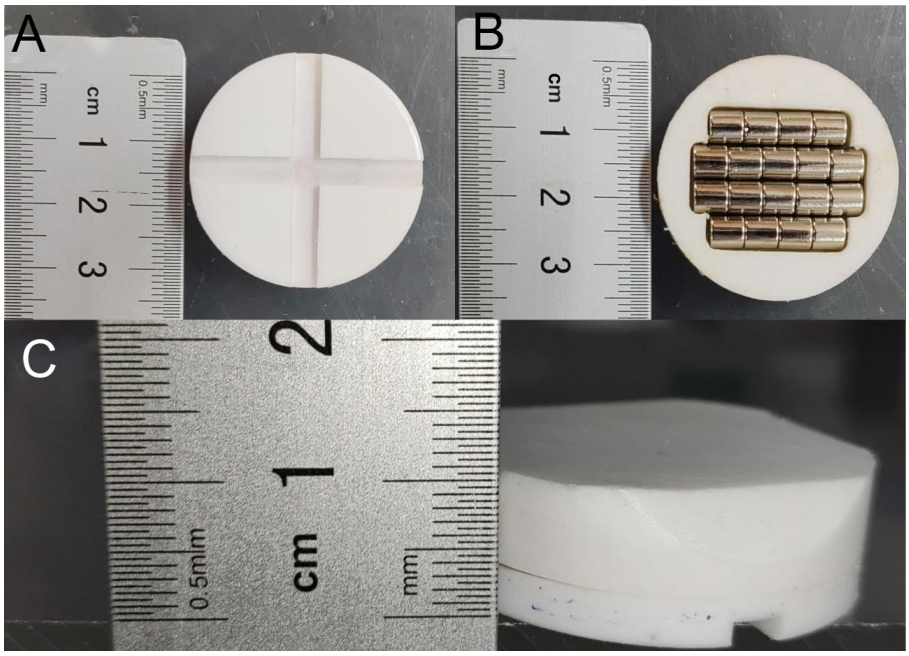

Figure 4. Photographs of a homemade PTFE magnetic rotary disk: (A) front surface with a cross-shaped groove; (B) back cover with 18 magnets mounted inside; (C) side view. (A-C) are reprinted with permission from[47]. Adhering to the CC BY 4.0 agreement. PTFE: Polytetrafluoroethylene.

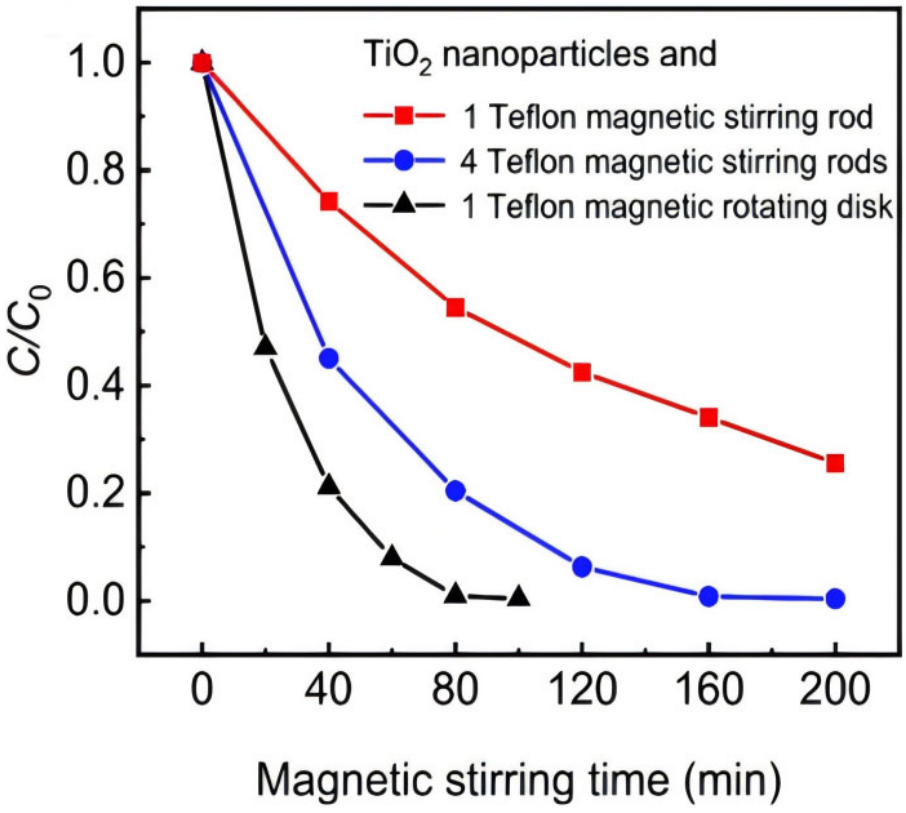

Figure 5. C/C_0 versus magnetic stirring time for 10 mg/L RhB solutions containing TiO_2 nanoparticles under magnetic stirring with one PTFE stirring rod, four PTFE stirring rods, or one PTFE magnetic rotary disk. Adapted with permission from[38]. Copyright 2022 Elsevier. PTFE: Polytetrafluoroethylene.

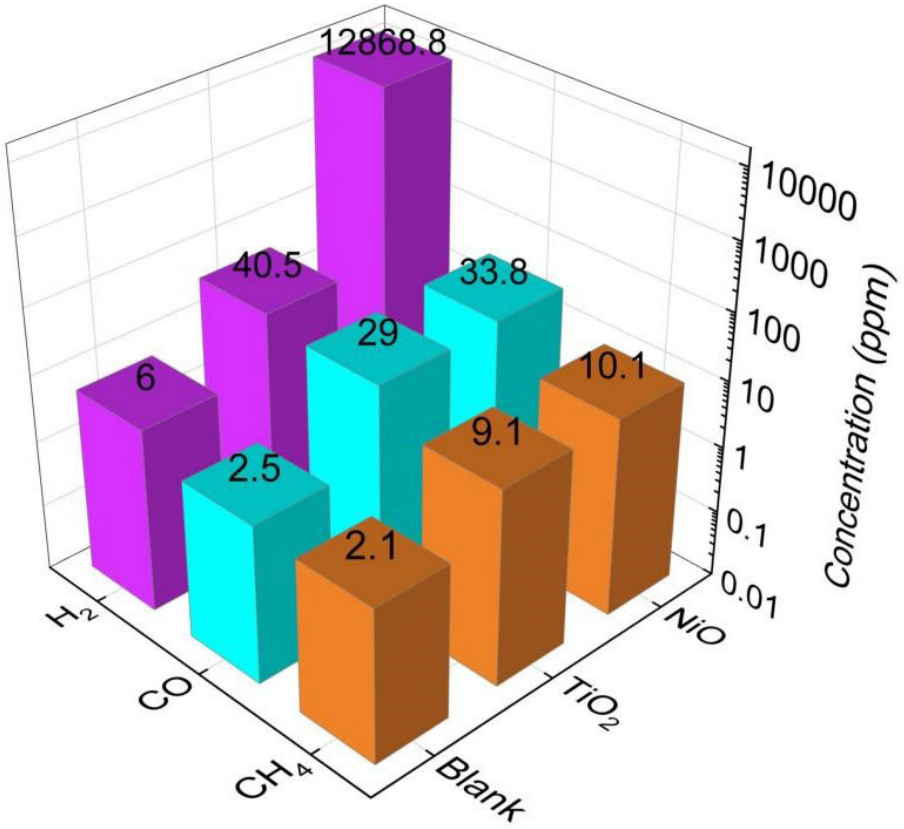

Figure 6. Production of flammable gases from H_2O and CO_2 in a glass reactor after 24 h of magnetic stirring with a PTFE magnetic rotary disk under three conditions: no particles, 1.00 g of TiO_2 nanoparticles, or 1.0 g of NiO particles. Reprinted with permission from[56]. Adhering to the CC BY 4.0 agreement. PTFE: Polytetrafluoroethylene.

mechanocatalytic overall water-splitting behavior of NiO reported by Ikeda *et al.* in 1999[59]. The origin of the enormous difference in H_2 production between TiO_2 and NiO remains unclear. Nevertheless, these results demonstrate the importance of PTFE magnetic rotary disks for tribocatalytic conversion of H_2O and CO_2 into flammable gases.

In most mechanochemical processes, mechanically induced heating must be considered[22-24], which complicates mechanistic analysis. For example, in the mechanocatalytic overall water-splitting system reported by Ikeda *et al.*, substantial H_2 production was observed for both NiO and Co_3O_4[59], but the proposed mechanocatalytic mechanism was questioned because magnetic stirring with PTFE magnetic rods at 1,500 rpm was believed to cause a large temperature rise[60]. Magnetic rotary disks, by contrast, typically operate at much lower speeds, such as 400 rpm, while still producing strong tribocatalytic effects[45]. As shown in Figure 7, H_2 production from H_2O after 1 h magnetic stirring using friction pairs of Co_3O_4/glass, Co_3O_4/Ti, and Al_2O_3/Si with PTFE magnetic rotary disks at 400 rpm was comparable to that obtained for NiO/glass and Co_3O_4/glass using PTFE magnetic rods at 1,500 rpm[61]. At this lower rotational speed, no obvious heating is observed during magnetic stirring, suggesting that magnetic rotary disks provide a particularly suitable mechanical-energy source for mechanistic studies of mechanochemistry in solutions.

It should be emphasized that rotational speed is an operating parameter rather than a direct measure of mechanical energy. Quantitative mechanical-energy input would additionally require information such as torque or friction force, contact conditions, and device geometry; therefore, absolute mechanical energy is not assigned when it was not measured in the original studies.

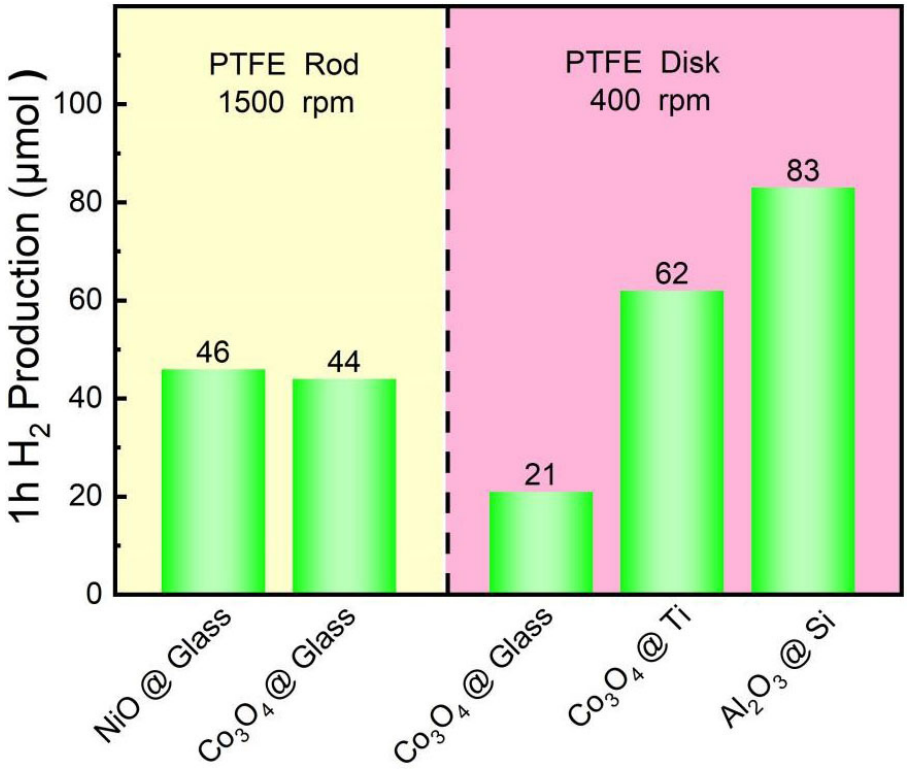

Figure 7. Comparison of H_2 production after 1 h magnetic stirring for several friction pairs. A PTFE magnetic rod rotating at 1500 rpm was used for NiO/glass and Co_3O_4/glass, whereas a PTFE magnetic rotary disk rotating at 400 rpm was used for Co_3O_4/glass, Co_3O_4/Ti, and Al_2O_3/Si. Reprinted with permission from[61]. Adhering to the CC BY 4.0 agreement. PTFE: Polytetrafluoroethylene.

Catalyst optimization

Because tribocatalysis is a form of heterogeneous catalysis in solution, substantial effort has been devoted to optimizing the catalysts themselves. A wide range of materials have been evaluated for tribocatalytic activity, and several important systems, including TiO_2, ZnO, $SrTiO_3$, and $BaTiO_3$, have been deliberately modified to improve their performance. Reported approaches include doping[41,49], heterojunction formation[43,62,63], thermal treatment in hydrogen[46], and morphology control[48,50,51]. These strategies are already well established in photocatalysis and are likely to remain important avenues for the future development of tribocatalysts.

For photocatalysts, a high specific surface area is generally considered essential for superior catalytic performance. Tribocatalysts, however, can exhibit a distinctly different trend.

Figure 8A, for example, compares the degradation of 5 mg/L RhB under identical conditions using three nanostructured ZnO samples: ZnO-1, ZnO-2, and ZnO-3[42]. Among them, ZnO-3 exhibited the highest tribocatalytic activity. As shown in Figure 8B, ZnO-3 is composed of much larger grains and has a lower specific surface area than ZnO-1 and ZnO-2. This trend contrasts sharply with the conventional behavior expected in photocatalysis.

To explain this behavior, high crystallinity has been proposed as a key property of semiconductor tribocatalysts because it facilitates the transport of friction-excited electron-hole pairs[64]. Similar trends have since been reported in multiple tribocatalysis studies, indirectly supporting the mechanism based on friction-induced carrier excitation in semiconductors. These findings suggest that catalyst-optimization principles in tribocatalysis can differ fundamentally from those in photocatalysis.

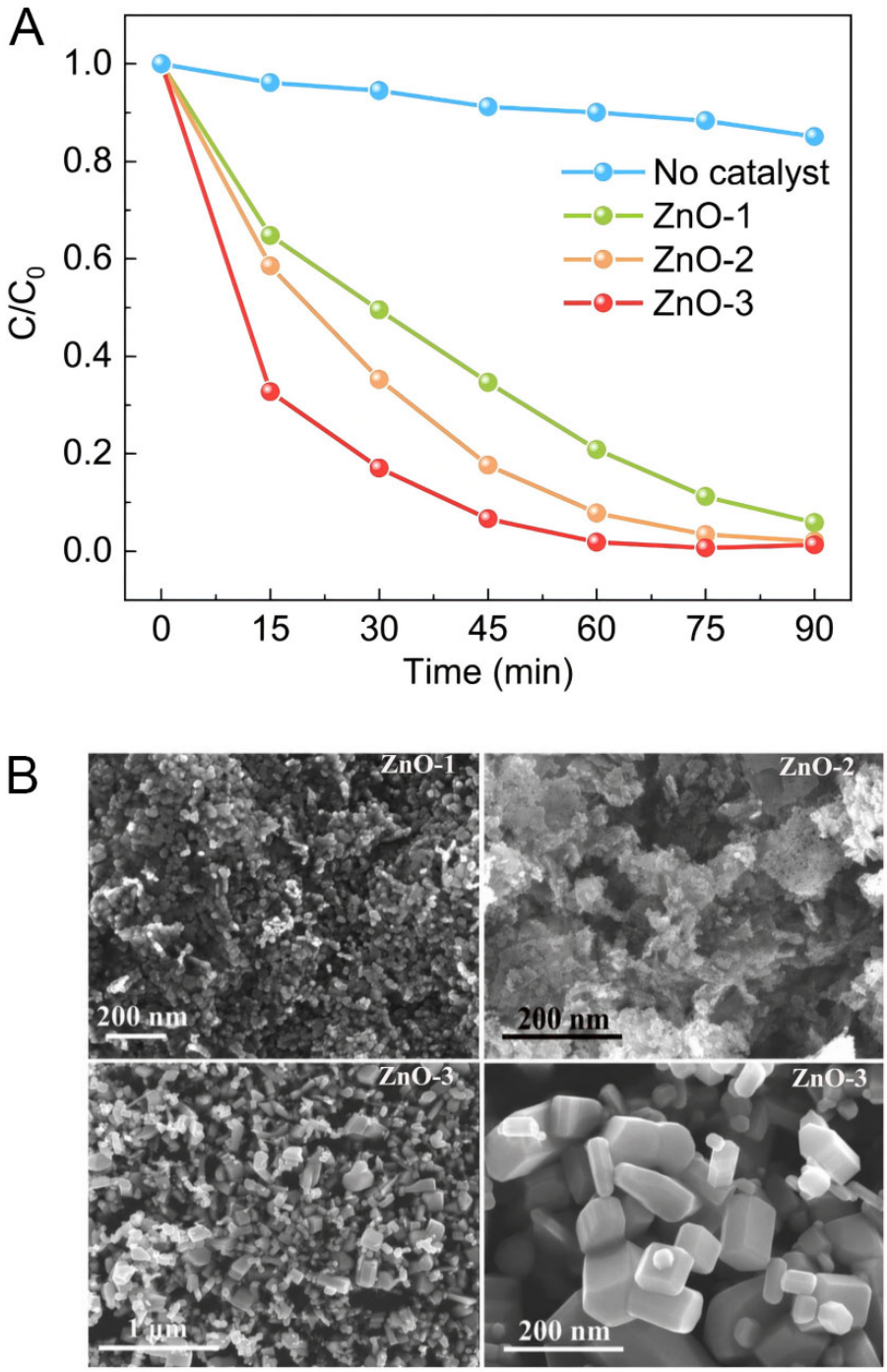

Figure 8. (A) RhB degradation efficiencies under magnetic stirring with three ZnO nanoparticle samples (ZnO-1, ZnO-2, and ZnO-3); (B) SEM images of ZnO-1, ZnO-2, and ZnO-3. (A and B) are adapted with permission from[42]. Adhering to the CC BY 4.0 agreement. SEM: Scanning electron microscopy.

Coating materials on vessel bottoms

Unlike photocatalysis, tribocatalysis offers an additional broadly effective enhancement strategy: coating disk-shaped materials onto the bottoms of vessels containing solutions[65]. This simple approach has played a critical role in several striking tribocatalytic results. For example, when high-concentration RhB solutions were treated with magnetic stirring-stimulated TiO_2 nanoparticles in beakers with glass, Al_2O_3, PTFE, or Ti bottoms, while 100 and 200 mg/L RhB solutions could be degraded within relatively short times with all four

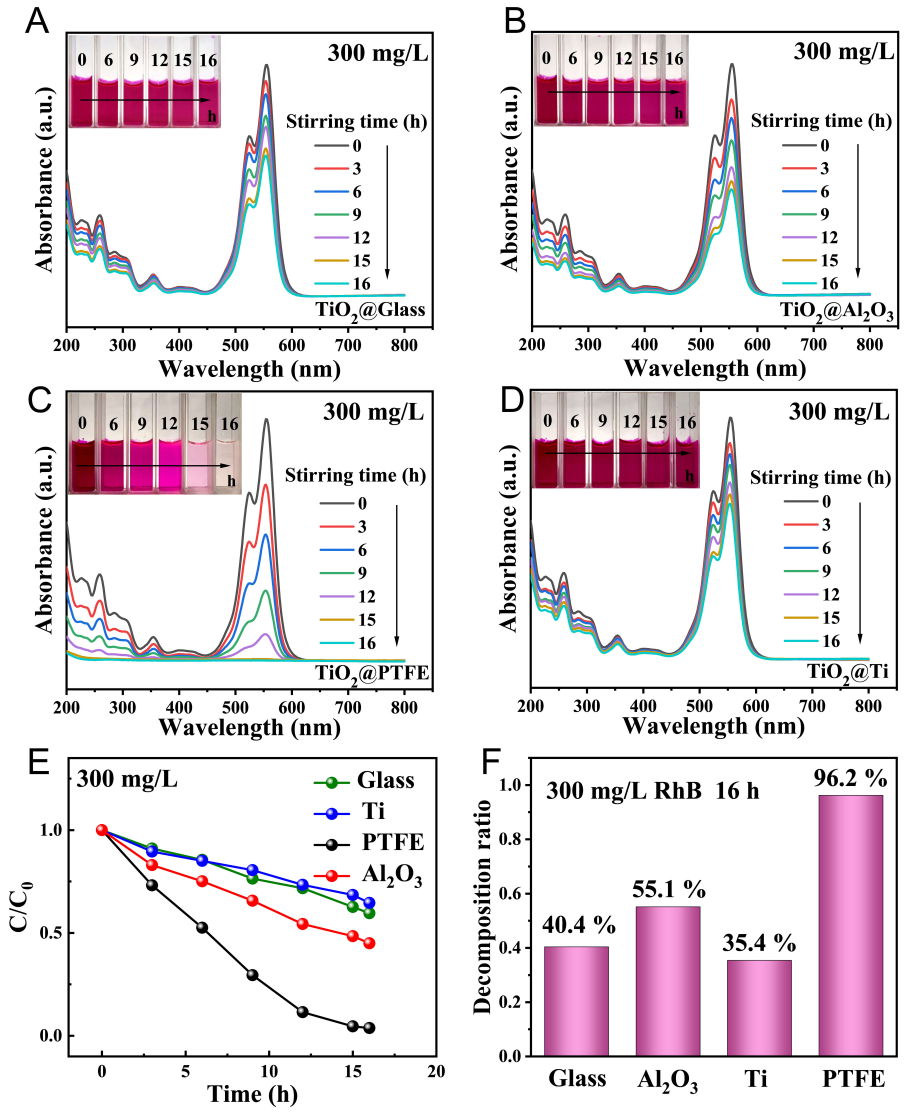

Figure 9. UV-Vis absorption spectra and color changes of 300 mg/L RhB solutions containing TiO_2 nanoparticles during magnetic stirring in beakers with (A) a glass bottom, (B) an Al_2O_3 coating, (C) a PTFE coating, and (D) a Ti coating; (E) C/C_0 as a function of magnetic stirring time; (F) degradation efficiencies after 16 h of magnetic stirring. (A-F) are reprinted with permission from[40]. Adhering to the CC BY 4.0 agreement. PTFE: Polytetrafluoroethylene; UV-Vis: ultraviolet-visible.

bottom materials[40], 300 mg/L RhB solution could be degraded in a relatively short time only with the PTFE bottom, as shown in Figure 9. In fact, 400 and 500 mg/L RhB solutions could still be efficiently degraded with the PTFE bottom. This enhancement associated with the PTFE bottom can be satisfactorily explained by the strong electron affinity of PTFE, which promotes separation of the electron-hole pairs excited in TiO_2 nanoparticles:

$$\mathrm{TiO_2NP} \xrightarrow{\text{Friction}} \mathrm{TiO_2NP \cdot\ h^+ \cdot e^-} \tag{2}$$

$$\mathrm{TiO_2NP \cdot\ h^+ \cdot e^- + PTFE} \xrightarrow{\text{Friction}} \mathrm{TiO_2NP \cdot\ h^+ + PTFE \cdot e^-} \tag{3}$$

The effects of bottom coatings, however, can be difficult to rationalize. As shown in Figure 10[55], when Co_3O_4 particles suspended in water containing CO_2 were stimulated by magnetic stirring with a PTFE magnetic rotary disk, a Ti-coated bottom increased H_2 and CH_4 production by factors of 1.87 and 26.4, respectively.

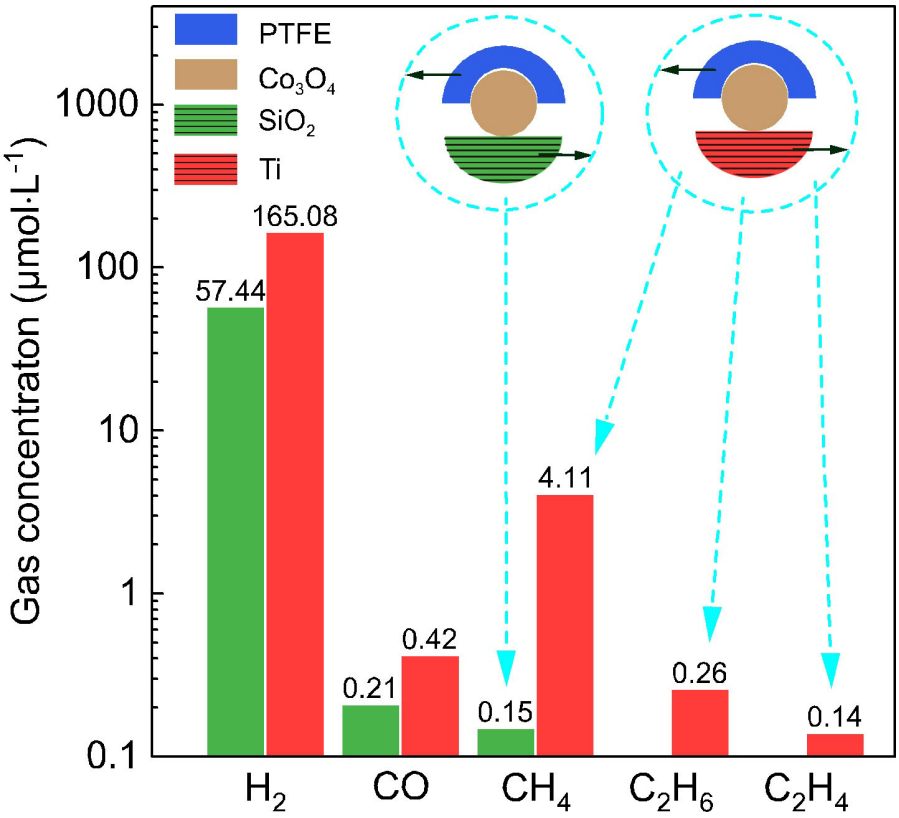

Figure 10. Tribocatalytic conversion of CO_2 and H_2O into flammable gases by Co_3O_4 in reactors with glass or Ti bottoms. Reprinted with permission from[55]. Adhering to the CC BY 4.0 agreement. PTFE: Polytetrafluoroethylene.

The Ti coating also enabled the formation of C_2H_6 and C_2H_4. In catalytic CO_2 conversion in water, CO_2 reduction typically competes with H_2 evolution, and the formation of C_2^+ products is particularly challenging. Although the origin of this effect remains unclear, the result highlights the attractive potential of tribocatalytic CO_2 conversion. Given its simplicity and effectiveness, vessel-bottom coating should be more broadly explored in tribocatalytic systems.

Coupling with other technologies

As an emerging technology, tribocatalysis has also been combined with established catalytic approaches. Several groups have investigated synergistic combinations of tribocatalysis with photocatalysis[66-68] and pyrocatalysis[44], with encouraging results. In our view, however, the most promising result to date is the coupling of tribocatalysis with PMS-based advanced oxidation processes (AOPs). As shown in Figure 11A-D, the degradation of 20 mg/L bisphenol A (BPA) and phenol by magnetic stirring-stimulated TiO_2 nanoparticles is greatly enhanced by the addition of PMS[69]. Compared with other methods used to activate peroxymonosulfate/peroxydisulfate (PMS/PDS), including heating, irradiation, and ultrasound[70,71], the rotary-disk approach used in this study is more readily scalable and therefore offers promise for large-scale PMS/PDS applications.

TRIBOCATALYSIS OF METALS IN AQUEOUS SOLUTIONS

Unlike semiconductors, for which tribocatalysis was first identified in aqueous systems, metallic materials were already known to exhibit mechanocatalytic activity[72,73]. In particular, certain metals can mechanically catalyze reactions between solids when used as milling balls or milling vessels in ball-milling processes, an approach termed direct mechanocatalysis[10,74]. Soon after tribocatalysis was identified in semiconductor

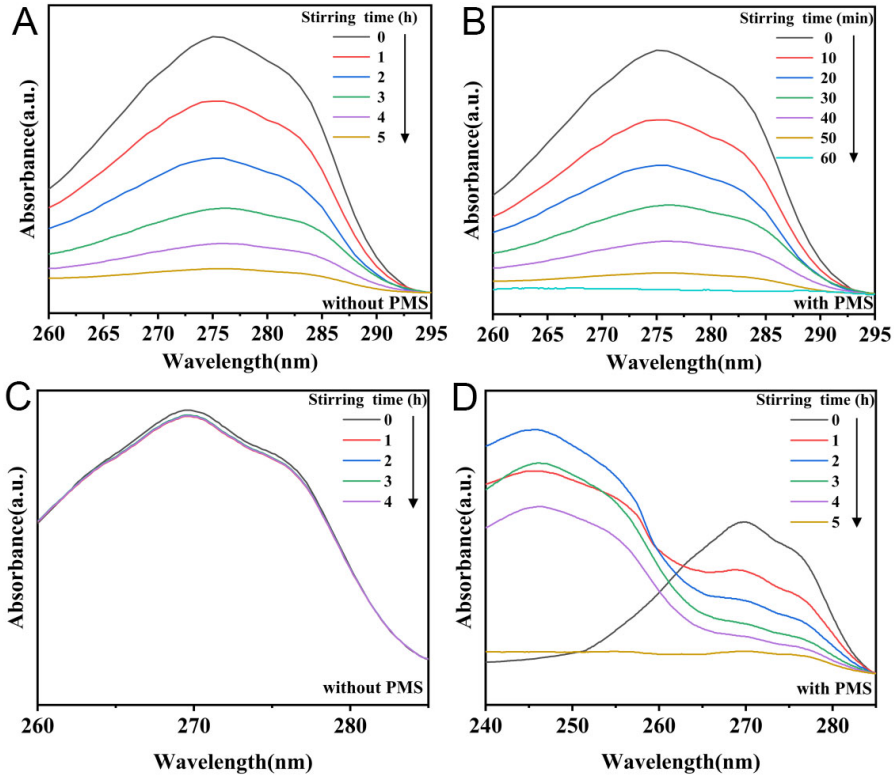

Figure 11. UV-Vis absorption spectra for the degradation of BPA and phenol by TiO_2 nanoparticles under magnetic stirring: (A) 20 mg/L BPA; (B) 20 mg/L BPA with 200 mg/L PMS; (C) 20 mg/L phenol; (D) 20 mg/L phenol with 200 mg/L PMS. (A-D) are reprinted with permission from[69]. Adhering to the CC BY 4.0 agreement. PMS: Peroxymonosulfate; BPA: bisphenol A; UV-Vis: ultraviolet-visible.

materials in aqueous solutions, analogous tribocatalytic behavior was also reported for metals[75].

Magnetic stirring with magnetic rotary disks has been instrumental in revealing the tribocatalysis of metals in aqueous solutions. Following the design of the PTFE magnetic rotary disk shown in Figure 4, metallic magnetic rotary disks were fabricated. As shown in Figure 12, four Ti disks (10 mm in diameter) were mounted on a larger PTFE disk (35 mm in diameter), with 18 magnets installed inside using the same design as the PTFE magnetic rotary disk[76]. When placed in a beaker on a conventional magnetic stirrer, the resulting Ti magnetic rotary disk rotates against the beaker bottom, producing dynamic friction at the Ti-bottom interface. Replacing the Ti disks with other metals, such as Cu, Ni, Ag, or Pb, readily produces corresponding metallic rotary disks and allows analogous metal-bottom friction pairs to be investigated[75].

Five types of metallic magnetic rotary disks - Cu, Ni, Ti, Ag, and Pb - were separately rotated in reactors containing H_2O and CO_2[75]. Although H_2, CO, and CH_4 were detected in all cases, H_2 production from Cu, Ni, and Ti exceeded that from Ag and Pb by more than two orders of magnitude. Accordingly, Cu, Ni, and Ti were classified as tribocatalytically active, whereas Ag and Pb were regarded as inert. The tribocatalytic conversion of H_2O and CO_2 can also be strongly regulated by the material coating the reactor bottom. For a Ni magnetic rotary disk, for example, Figure 13 shows the gas products obtained with different coatings[77]. A glass bottom gave the highest absolute yields of H_2 and CH_4, whereas a Ni-coated bottom produced the highest CH_4/H_2 and C_2H_6/H_2 ratios; C_2H_4 was detected only with a Ti-coated bottom. These results reveal substantial potential for using low-frequency friction with metallic materials to convert H_2O and CO_2 into flammable gases.

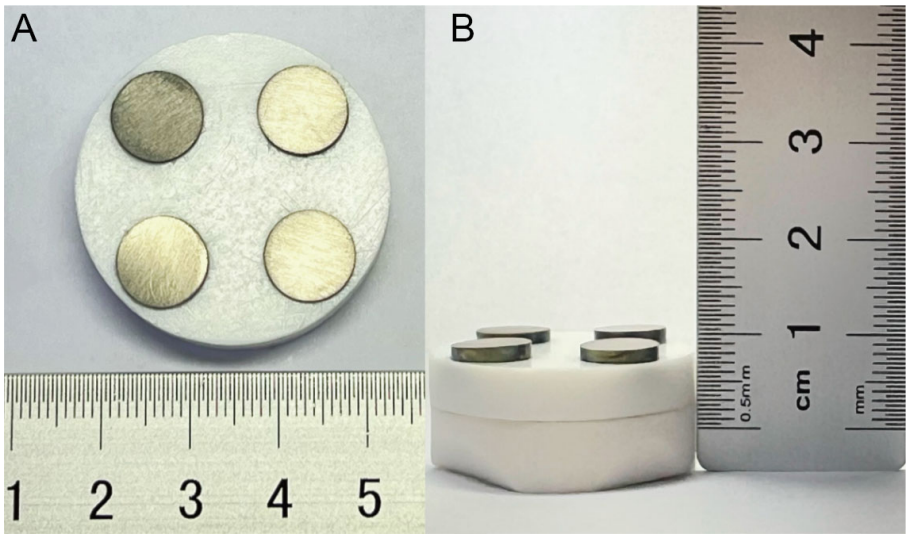

Figure 12. Images of a Ti magnetic rotary disk: (A) front surface; (B) side surface. (A and B) are reprinted with permission from[76]. Adhering to the CC BY 4.0 agreement.

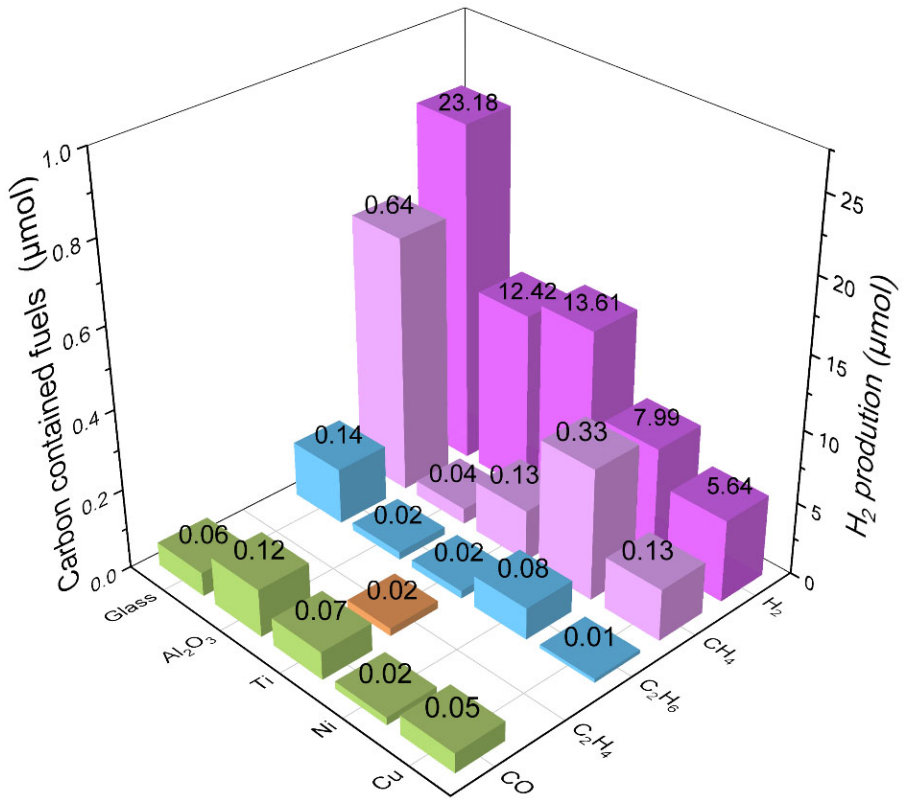

Figure 13. Flammable gases produced after 5 h of magnetic stirring with a Ni magnetic rotary disk in reactors containing H_2O and CO_2 and equipped with glass, Al_2O_3, Ti, Ni, or Cu bottoms. Reprinted with permission from[77]. Copyright 2024 Elsevier.

In one study of five metals (Cu, Ni, Ti, Ag, and Pb), three - Cu, Ni, and Ti - were found capable of mechanically catalyzing the conversion of H_2O and CO_2[75]. The apparent generality of this behavior motivated a relatively simple mechanism for metal tribocatalysis. Taking a Ni magnetic rotary disk in water as an example[77], magnetic stirring generates dynamic friction between the Ni disk and the reactor bottom, whether glass [Figure 14A] or Ni [Figure 14B]. Because the friction surfaces are microscopically rough, water

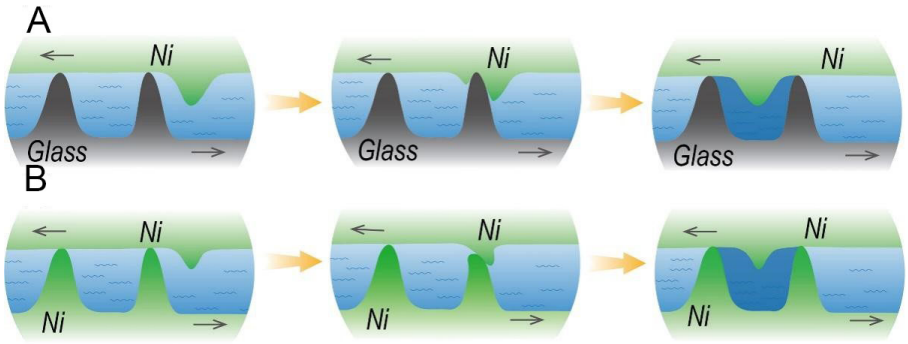

Figure 14. Schematic illustrations of water blocking and squeezing in microholes by a Ni magnetic rotary disk under magnetic stirring: (A) on a glass bottom; (B) on a Ni bottom. (A and B) are reprinted with permission from[77]. Copyright 2024 Elsevier.

can become trapped in surface micro-holes and compressed through the elastic deformation of Ni. Under the resulting elevated local pressure, Ni, as well as Cu and Ti[75], can catalyze the conversion of H_2O and CO_2 trapped in these micro-holes. By contrast, Ag and Pb exhibit no catalytic activity under the same conditions, indicating intrinsic differences among metals in their catalytic behavior at high pressure. Importantly, this mechanism provides a second pathway - distinct from semiconductor tribocatalysis - by which friction can convert mechanical energy into chemical energy without relying on bulk heating or bond breaking in the solid. This absorption of frictional energy through elastic deformation lays the foundation for metal tribocatalysis, although it still requires more direct quantitative verification of the interfacial pressure and deformation.

In photocatalytic and electrocatalytic conversion of H_2O and CO_2, the catalysts are typically nanostructured materials, and their long-term stability remains a major barrier to practical application. By contrast, the ability of bulk metals to catalyze the conversion of H_2O and CO_2 into flammable gases under low-frequency friction[75,77] suggests that metal tribocatalysis could provide a robust approach for large-scale H_2O and CO_2 conversion. This area therefore warrants much broader investigation, particularly for the conversion of H_2O and CO_2.

It is useful to compare tribocatalysis in semiconductors and metallic materials. First, semiconductors absorb frictional energy by exciting electron-hole pairs, whereas metallic materials absorb it through elastic deformation. Second, semiconductor tribocatalysis arises from the combined action of electrons, holes, and the reactive radicals they generate, whereas metallic-material tribocatalysis exploits the intrinsic catalytic activity of the metal under elevated local pressure. These two classes of tribocatalysis therefore differ fundamentally in mechanism. In terms of applications, semiconductor tribocatalysis is highly versatile and may be applicable to many processes conventionally addressed by photocatalysis, whereas metallic-material tribocatalysis appears particularly promising for H_2O and CO_2 conversion[75-77]. Because tribocatalysis is application-oriented, selecting the appropriate material is of primary importance.

For convenient comparison, Table 1 summarizes several representative systems for which this mini-review has collected sufficient information on device, mechanical-input conditions, performance, and reaction time.

CONCLUSION AND OUTLOOK

Since tribocatalytic degradation of organic dyes was first reported in 2019, the field has expanded rapidly, generating numerous studies of environmentally relevant reactions driven by mechanical energy. Beyond organic-pollutant degradation and the conversion of CO_2 and H_2O, proposed applications now include N_2 fixation[78], H_2O_2 synthesis[79], Li-ion battery recovery[80], uranium extraction[81], and bacterial sterilization[82].

Table 1. Representative tribocatalytic systems discussed in this mini-review

Catalyst/system	Device and mechanical-input information	Application	Performance/yield	Time	Mechanistic interpretation
BST nanoparticles[21]	Magnetic stirring with PTFE rod; absolute mechanical energy not quantified	RhB degradation	5 mg/L RhB degraded under the reported conditions	12 h	Friction-excited electron-hole pairs and radical formation
TiO_2 nanoparticles[58]	Four PTFE magnetic rods; absolute mechanical energy not quantified	H_2O/CO_2 conversion	8.98 ppm H_2; 2.61 ppm CH_4; 30.04 ppm CO	50 h	Semiconductor carrier-mediated redox pathway
TiO_2 nanoparticles[56]	PTFE magnetic rotary disk; absolute mechanical energy not quantified	H_2O/CO_2 conversion	40.5 ppm H_2; 9.1 ppm CH_4; 29 ppm CO	24 h	Semiconductor carrier-mediated redox pathway
NiO particles[56]	PTFE magnetic rotary disk; absolute mechanical energy not quantified	H_2 production from $H_2O + CO_2$	12,868.8 ppm H_2	24 h	Friction-induced electronic processes discussed for semiconductor tribocatalysis
TiO_2 + PTFE-bottom reactor[40]	Magnetic stirring with PTFE friction interface; absolute mechanical energy not quantified	High-concentration RhB degradation	300 mg/L RhB degraded by 96.2%	16 h	PTFE promotes separation of friction-excited charge carriers

BST: $Ba_{0.75}Sr_{0.25}TiO_3$; PTFE: Polytetrafluoroethylene.

At the same time, important mechanistic insights have emerged into the direct conversion of mechanical energy into chemical energy through friction in solutions, and several broadly effective strategies for enhancing and regulating tribocatalysis have been established. Tribocatalysis is therefore expected to continue developing as an important tool for sustainable technologies.

Despite the growing number of studies on this emerging form of heterogeneous catalysis in aqueous solutions, many investigations have not yet incorporated the most effective design principles established in the field. For example, conventional magnetic stirring with a commercial PTFE magnetic rod is still widely used for tribocatalytic degradation of organic pollutants, even though its degradation efficiency is substantially lower than that achieved with the PTFE magnetic rotary disk introduced in 2022[38]. Similarly, coatings on vessel bottoms have been shown to strongly influence tribocatalysis in many systems[65], yet they remain unexplored in most current studies. Because tribocatalysis fundamentally depends on dynamic friction, future studies should continue to optimize the friction interface, while also improving the quantitative characterization of mechanical-energy input and standardizing reporting of device geometry and operating conditions. More direct mechanistic measurements, targeting organic pollutants beyond model dyes, evaluating energy efficiency, and scaling up will all be important for practical development.

DECLARATIONS

Authors' contributions

Completed the main writing of the manuscript: Zhou, Z.
Collected and integrated the relevant references: Yao, W.
Designed the manuscript outline, offered professional guidance, and revised the initial draft: Chen, W.

Availability of data and materials

Not applicable.

AI and AI-assisted tools statement

Not applicable.

Financial support and sponsorship

None.

Conflicts of interest

All authors declare that there are no conflicts of interest.

Ethical approval and consent to participate

Not applicable.

Consent for publication

Not applicable.

Copyright

REFERENCES

1. Gaudino E, Cravotto G, Manzoli M, Tabasso S. Sono- and mechanochemical technologies in the catalytic conversion of biomass. *Chem. Soc. Rev.* **2021**, *50*, 1785-812. DOI PubMed
2. Hergesell, A. H.; Baarslag, R. J.; Seitzinger, C. L.; et al. Surface-activated mechano-catalysis for ambient conversion of plastic waste. *J. Am. Chem. Soc.* **2024**, *146*, 26139-47. DOI PubMed PMC
3. Gilman, J. J. Mechanochemistry. *Science* **1996**, *274*, 65-65. DOI
4. Dong, L.; Li, L.; Chen, H.; Cao, Y.; Lei, H. Mechanochemistry: fundamental principles and applications. *Adv. Sci. (Weinh).* **2025**, *12*, e2403949. DOI PubMed PMC
5. Baláž, P.; Achimovičová, M.; Baláž, M.; et al. Hallmarks of mechanochemistry: from nanoparticles to technology. *Chem. Soc. Rev.* **2013**, *42*, 7571-637. DOI
6. Takacs, L. The historical development of mechanochemistry. *Chem. Soc. Rev.* **2013**, *42*, 7649-59. DOI PubMed
7. Heinicke, G. Tribochemistry. Akademie-Verlag: Berlin, 1984. https://books.google.com/books/about/Tribochemistry.html?id=ZfQ_EQAAQBAJ (accessed 2026-9-28).
8. Muratov, V.; Luangvaranunt, T.; Fischer, T. The tribochemistry of silicon nitride: effects of friction, temperature and sliding velocity. *Tribol. Int.* **1998**, *31*, 601-11. DOI
9. Hermann, G. N.; Becker, P.; Bolm, C. Mechanochemical iridium(III)-catalyzed C-H bond amidation of benzamides with sulfonyl azides under solvent-free conditions in a ball mill. *Angew. Chem. Int. Ed. Engl.* **2016**, *55*, 3781-4. DOI
10. Pickhardt, W.; Kraus, F. J. L.; Wohlgemuth, M.; et al. Direct mechanocatalysis with Pd alloys. *ChemCatChem* **2024**, *16*, e202400491. DOI
11. Wohlgemuth, M.; Schmidt, S.; Mayer, M.; Pickhardt, W.; Graetz, S.; Borchardt, L. Solid-state oxidation of alcohols in gold-coated milling vessels via direct mechanocatalysis. *Angew. Chem. Int. Ed. Engl.* **2024**, *63*, e202405342. DOI PubMed
12. 12 Kajdas, C.; Hiratsuka, K., Eds. Tribocatalysis, tribochemistry, and tribocorrosion; Pan Stanford Publishing: Singapore, 2018. DOI
13. Onodera, T.; Kawasaki, K.; Nakakawaji, T.; et al. Tribocatalytic reaction of polytetrafluoroethylene sliding on an aluminum surface. *J. Phys. Chem. C.* **2015**, *119*, 15954-62. DOI
14. Franco, A.; Jérôme, F.; De, Oliveira. Vigier. K. Mechanocatalysis: background and challenges. *npj. Mater. Sustain.* **2026**, *4*, 105. DOI
15. Hick, S. M.; Griebel, C.; Restrepo, D. T.; et al. Mechanocatalysis for biomass-derived chemicals and fuels. *Green. Chem.* **2010**, *12*, 468. DOI
16. Luterbacher, J. S.; Martin, Alonso. D.; Dumesic, J. A. Targeted chemical upgrading of lignocellulosic biomass to platform molecules. *Green. Chem.* **2014**, *16*, 4816-38. DOI
17. Kleine, T.; Buendia, J.; Bolm, C. Mechanochemical degradation of lignin and wood by solvent-free grinding in a reactive medium. *Green. Chem.* **2013**, *15*, 160-6. DOI
18. Berman, D.; Erdemir, A. Achieving ultralow friction and wear by tribocatalysis: enabled by in-operando formation of nanocarbon films. *ACS. Nano.* **2021**, *15*, 18865-79. DOI PubMed
19. Song, W.; Li, J.; Zeng, C.; et al. Tribo-catalysis triggered the in-situ formation of amphiphilic molecules to reduce friction and wear. *Tribol. Int.* **2023**, *185*, 108541. DOI
20. Berman, D.; Erdemir, A. The role of tribocatalysis in friction and wear: a review. *Lubricants* **2025**, *13*, 442. DOI
21. Li, P.; Wu, J.; Wu, Z.; et al. Strong tribocatalytic dye decomposition through utilizing triboelectric energy of barium strontium titanate nanoparticles. *Nano. Energy.* **2019**, *63*, 103832. DOI
22. Burmeister, C. F.; Kwade, A. Process engineering with planetary ball mills. *Chem. Soc. Rev.* **2013**, *42*, 7660-7. DOI PubMed
23. Tricker, A. W.; Samaras, G.; Hebisch, K. L.; Realff, M. J.; Sievers, C. Hot spot generation, reactivity, and decay in mechanochemical reactors. *Chem. Eng. J.* **2020**, *382*, 122954. DOI

24. Delogu, F.; Cocco, G. Weakness of the “hot spots” approach to the kinetics of mechanically induced phase transformations. *J. Alloys. Compd.* **2008**, *465*, 540-6. DOI
25. Friščić, T.; Halasz, I.; Beldon, P. J.; et al. Real-time and in situ monitoring of mechanochemical milling reactions. *Nat. Chem.* **2013**, *5*, 66-73. DOI
26. Gracin, D.; Štrukil, V.; Friščić, T.; Halasz, I.; Užarević, K. Laboratory real-time and *in situ* monitoring of mechanochemical milling reactions by Raman spectroscopy. *Angew. Chem. Int. Ed. Engl.* **2014**, *53*, 6193-7. DOI PubMed
27. Michalchuk, A. A. L.; Emmerling, F. Time-resolved in situ monitoring of mechanochemical reactions. *Angew. Chem. Int. Ed. Engl.* **2022**, *61*, e202117270. DOI PubMed PMC
28. Mateti, S.; Mathesh, M.; Liu, Z.; et al. Mechanochemistry: a force in disguise and conditional effects towards chemical reactions. *Chem. Commun. (Camb).* **2021**, *57*, 1080-92. DOI
29. Mckissic, K. S.; Caruso, J. T.; Blair, R. G.; Mack, J. Comparison of shaking versus baking: further understanding the energetics of a mechanochemical reaction. *Green. Chem.* **2014**, *16*, 1628. DOI
30. Meng, Q.; Shao, M.; Su, H.; et al. Influence of humidity on the tribological properties of PTFE/Al_2O_3 and PTFE/SiO_2 composites: an interpretation based on the tribocatalysis mechanism. *Tribol. Int.* **2026**, *219*, 111820. DOI
31. Nadeem, I.; Finšgar, M.; Dražić, G.; et al. Macroscale superlubricity with a high load-carrying capacity enabled by nitrogen-doped graphene quantum dots in lubricated silicon-doped amorphous carbon films. *Small. Struct.* **2025**, *6*, 2400671. DOI
32. Xu, Y.; Li, S.; Zhong, H.; Hu, K.; Ren, T. Highly graphitized carbonaceous transfer tribofilms tribo-catalyzed by slightly water-soluble additives for reducing friction and wear of polylactic acid. *Tribol. Int.* **2026**, *218*, 111715. DOI
33. Feng, Y.; Ling, L.; Wang, Y.; et al. Engineering spherical lead zirconate titanate to explore the essence of piezo-catalysis. *Nano. Energy.* **2017**, *40*, 481-6. DOI
34. Zhu, R.; Xu, Y.; Bai, Q.; Wang, Z.; Guo, X.; Kimura, H. Direct degradation of dyes by piezoelectric fibers through scavenging low frequency vibration. *Chem. Phys. Lett.* **2018**, *702*, 26-31. DOI
35. Liu, X.; Shen, L.; Xu, W.; et al. Low frequency hydromechanics-driven generation of superoxide radicals via optimized piezotronic effect for water disinfection. *Nano. Energy.* **2021**, *88*, 106290. DOI
36. Cui, X.; Guo, Z.; Lei, H.; et al. Tribo-catalytic degradation of methyl orange solutions enhanced by silicon single crystals. *Coatings* **2023**, *13*, 1804. DOI
37. Li, P.; Tang, C.; Cheng, L.; Hu, Y.; Xiao, X.; Chen, W. Reduction of CO_2 by TiO_2 nanoparticles through friction in water. *Acta. Phys. Sin.* **2021**, *70*, 214601. DOI
38. Cui, X.; Li, P.; Lei, H.; et al. Greatly enhanced tribocatalytic degradation of organic pollutants by TiO_2 nanoparticles through efficiently harvesting mechanical energy. *Sep. Purif. Technol.* **2022**, *289*, 120814. DOI
39. Molla, R.; Aktar, S.; Roy, S. S.; Alam, N.; Tamang, A.; Chattopadhyay, B. TiO_2 incorporated polystyrene composites for triboelectric nanogenerator applications and tribo-catalytic dye degradation. *Colloids. Surf. A:. Physicochem. Eng. Asp.* **2026**, *746*, 140763. DOI
40. Gu, Y.; Cheng, X.; Wang, R.; et al. PTFE-enhanced tribocatalytic degradation of high-concentration (100-500 mg/L) rhodamine B solutions using TiO_2 nanoparticles. *Coatings* **2026**, *16*, 111. DOI
41. Hu, J.; Ma, W.; Pan, Y.; et al. Insights on the mechanism of Fe doped ZnO for tightly-bound extracellular polymeric substances tribo-catalytic degradation: the role of hydration layers at the interface. *Chemosphere* **2021**, *276*, 130170. DOI
42. Lei, H.; Cui, X.; Jia, X.; Qi, J.; Wang, Z.; Chen, W. Enhanced tribocatalytic degradation of organic pollutants by ZnO nanoparticles of high crystallinity. *Nanomaterials. (Basel).* **2022**, *13*, 46. DOI PubMed PMC
43. Ivanova, D.; Kolev, H.; Mladenova, R.; Stefanov, B. I.; Kaneva, N. Harvesting friction energy on zinc oxide and zinc oxide/europium oxide sol-gel catalysts for tribocatalytic paracetamol degradation. *Molecules* **2025**, *30*, 2265. DOI PubMed PMC
44. Yang, B.; Chen, H.; Yang, Y.; et al. Insights into the tribo-/pyro-catalysis using Sr-doped $BaTiO_3$ ferroelectric nanocrystals for efficient water remediation. *Chem. Eng. J.* **2021**, *416*, 128986. DOI
45. Gaur, A.; Porwal, C.; Chauhan, V. S.; Vaish, R. Tribocatalytic investigation of $BaTiO_3$ for dye removal from water. *J. Mater. Sci:. Mater. Electron.* **2023**, *34*, 11511. DOI
46. Geng, L.; Qian, Y.; Song, W.; Bao, L. Enhanced tribocatalytic pollutant degradation through tuning oxygen vacancy in $BaTiO_3$ nanoparticles. *Appl. Surf. Sci.* **2023**, *637*, 157960. DOI
47. Zhu, M.; Zhou, Z.; Gu, Y.; et al. Powerful tribocatalytic degradation of methyl orange solutions with concentrations as high as 100 mg/L by $BaTiO_3$ nanoparticles. *Nanomaterials. (Basel).* **2025**, *15*, 1135. DOI PubMed PMC
48. Cao, J.; Jia, Y.; Wan, X.; et al. Strong tribocatalysis of strontium titanate nanofibers through harvesting friction energy for dye decomposition. *Ceram. Int.* **2022**, *48*, 9651-7. DOI
49. Xu, Y.; Meng, Y.; Xiang, X.; et al. Modulating low-frequency tribocatalytic performance through defects in uni-doped and bi-doped $SrTiO_3$. *J. Adv. Ceram.* **2024**, *13*, 1153-63. DOI

50. Chen, B.; Cheng, C.; Xu, T.; et al. High tribocatalytic nitrogen fixation at friction interface between non-piezoelectric $SrTiO_3$ nanosheets and PTFE. *Surf. Interfaces.* **2025**, *65*, 106461. DOI
51. Yang, B.; Chen, H.; Guo, X.; et al. Enhanced tribocatalytic degradation using piezoelectric CdS nanowires for efficient water remediation. *J. Mater. Chem. C.* **2020**, *8*, 14845-54. DOI
52. Aktar, S.; Roy, S. S.; Paul, D.; Mridha, S.; Tamang, A.; Chattopadhyay, B. Tribo-catalytic dye-degrading and antibacterial performance of CdS quantum dot-incorporated polystyrene nanocomposite membrane. *Colloids. Surf. A:. Physicochem. Eng. Asp.* **2026**, *749*, 141257. DOI
53. Xu, X.; Mao, C.; Song, J.; et al. Surprising effects of Ti and Al_2O_3 coatings on tribocatalytic degradation of organic dyes by GaN nanoparticles. *Materials. (Basel).* **2024**, *17*, 3487. DOI PubMed PMC
54. Wang, Y.; Wu, Z.; Hong, S.; et al. Highly efficient tribocatalysis of superhard SiC for water purification. *Nanomaterials. (Basel).* **2025**, *15*, 1206. DOI PubMed PMC
55. Jia, X.; Wang, H.; Lei, H.; et al. Boosting tribo-catalytic conversion of H_2O and CO_2 by Co_3O_4 nanoparticles through metallic coatings in reactors. *J. Adv. Ceram.* **2023**, *12*, 1833-43. DOI
56. Lei, H.; Jia, X.; Wang, H.; et al. Tribo-catalytic conversions of H_2O and CO_2 by NiO particles in reactors with plastic and metallic coatings. *Coatings* **2023**, *13*, 396. DOI
57. Yu, H.; Fu, J.; Zhu, X.; et al. Tribocatalytic degradation of organic pollutants using Fe_2O_3 nanoparticles. *ACS. Appl. Nano. Mater.* **2023**, *6*, 14364-73. DOI
58. Li, P.; Tang, C.; Xiao, X.; Jia, Y.; Chen, W. Flammable gases produced by TiO_2 nanoparticles under magnetic stirring in water. *Friction* **2022**, *10*, 1127-33. DOI
59. Ikeda, S.; Takata, T.; Komoda, M.; et al. Mechano-catalysis - a novel method for overall water splitting. *Phys. Chem. Chem. Phys.* **1999**, *1*, 4485-91. DOI
60. Ross, D. S. Comment on “A study of mechano-catalysis for overall water splitting”. *J. Phys. Chem. B.* **2004**, *108*, 19076-7. DOI
61. Zhou, J.; Cui, X.; Zhang, J.; et al. Surprising tribocatalytic production of H_2 from H_2O by silicon single crystals via low-speed magnetic stirring. *Catalysts* **2026**, *16*, 523. DOI
62. Jin, Z.; Zheng, X.; Zhu, Z.; et al. Enhanced triboelectric degradation of organics by regulating oxygen vacancies and constructing heterojunctions. *Appl. Surf. Science.* **2023**, *625*, 157228. DOI
63. Wang, Y.; Shen, S.; Liu, M.; He, G.; Li, X. Enhanced tribocatalytic degradation performance of organic pollutants by $Cu_{1.8}S/CuCo_2S_4$ p-n junction. *J. Colloid. Interface. Sci.* **2024**, *655*, 187-98. DOI
64. Zhou, Z.; Luo, R.; Mao, C.; Hu, Y.; Chen, W. Contrasting tribocatalytic degradations of organic dyes by two different commercial silicon powders. *J. Adv. Dielect.* **2025**, *15*, 2450025. DOI
65. Mao, C.; Guo, Z.; Chen, W. Coating disk-shaped materials on the bottoms of vessels: a convenient while marvelous practice for tribocatalysis. *Surf. Interfaces.* **2025**, *60*, 106106. DOI
66. Wang, T.; Wei, Z.; Wang, X.; Zhang, L.; Zhao, W.; Yue, C. Oxygen-vacancy-engineered BiO_{2-x}/Bi_2O_3 heterojunctions for synergistic photo-tribocatalytic degradation and broad-spectrum antibacterial performance. *React. Chem. Eng.* **2026**, *11*, 731-45. DOI
67. Sharma, A. K.; Vaish, R.; Singh, G. Solar energy enhanced tribocatalytic dye degradation using high entropy perovskite ceramics. *Solar. Energy.* **2025**, *301*, 113906. DOI
68. Xu, Z.; Liu, C.; Cong, H.; Kong, Y.; Wang, P.; Li, X. Oxygen vacancy-engineered Z-scheme $Bi_2O_2CO_3/ZnFe_2O_4$ heterojunction for day-night tribo-photocatalytic removal of pollutants. *J. Environ. Chem. Eng.* **2025**, *13*, 118459. DOI
69. Zhou, Z.; Chen, R.; Zhu, H.; Hu, Y.; Li, N.; Chen, W. Tribocatalytic activation of peroxymonosulfate by TiO_2 nanoparticles for powerful degradation of organic pollutants. *J. Adv. Ceram.* **2026**, *15*, 9221237. DOI
70. Lee, J.; von, Gunten. U.; Kim, J. H. Persulfate-based advanced oxidation: critical assessment of opportunities and roadblocks. *Environ. Sci. Technol.* **2020**, *54*, 3064-81. DOI PubMed
71. Chen, Y.; Lan, S.; Zhu, M. Construction of piezoelectric $BaTiO_3/MoS_2$ heterojunction for boosting piezo-activation of peroxymonosulfate. *Chin. Chem. Lett.* **2021**, *32*, 2052-6. DOI
72. Sawama, Y.; Niikawa, M.; Sajiki, H. Stainless steel ball milling for hydrogen generation and its application for reduction. *J. Synth. Org. Chem. Jpn.* **2019**, *77*, 1070-7. DOI
73. Han, G. F.; Li, F.; Chen, Z. W.; et al. Mechanochemistry for ammonia synthesis under mild conditions. *Nat. Nanotechnol.* **2021**, *16*, 325-30. DOI
74. Pickhardt, W.; Grätz, S.; Borchardt, L. Direct mechanocatalysis: using milling balls as catalysts. *Chemistry* **2020**, *26*, 12903-11. DOI PubMed PMC

75. Cui, X.; Wang, H.; Lei, H.; et al. Surprising tribo-catalytic conversion of H_2O and CO_2 into flammable gases utilizing frictions of copper in water. *ChemistrySelect* **2023**, *8*, e202204146. DOI
76. Zhu, H.; Zhou, Z.; Ke, S.; Mao, C.; Song, J.; Chen, W. Tribocatalytic degradation of organic dyes by disk-shaped PTFE and titanium: a powder-free catalytic technology for wastewater treatment. *Catalysts* **2025**, *15*, 754. DOI
77. Lei, H.; Wu, Z.; Wang, H.; et al. Converting H_2O and CO_2 into chemical fuels by nickel via friction. *Surf. Interfaces.* **2024**, *46*, 104203. DOI
78. Wu, Z.; Xu, T.; Ruan, L.; et al. Strong tribocatalytic nitrogen fixation of graphite carbon nitride g-C_3N_4 through harvesting friction energy. *Nanomaterials. (Basel).* **2022**, *12*, 1981. DOI PubMed PMC
79. Sui, X.; Yang, Z.; Xiao, J.; et al. Highly efficient tribocatalytic hydrogen peroxide production over Fe_2O_3 nanoparticles and the reaction pathways. *J. Colloid. Interface. Sci.* **2026**, *720*, 140693. DOI
80. Jin, Z.; Su, B.; Wu, S.; et al. Tribocatalytic recycling of lithium-ion batteries. *J. Adv. Ceram.* **2025**, *14*, 9221121. DOI
81. Zhang, S.; Gao, F.; Fang, M.; et al. Catalyst-free extraction of U(VI) in solution by tribocatalysis. *Adv. Sci. (Weinh).* **2024**, *11*, e2404397. DOI PubMed PMC
82. Jin, Z.; Zheng, X.; Zhu, Z.; et al. Tribocatalytic sterilization of BN_2/CN Z-type heterojunctions. *Nano. Energy.* **2024**, *122*, 109284. DOI